BMB
Reports

BMB Rep. 2025; 58(2): 82-88
www.bmbreports.org

Role of histone modification in chromatin-mediated transcriptional repression in protozoan parasite *Trichomonas vaginalis*

Min-Ji Song[1,#], *Mikyoung Kim*[1,#], *Jieun Seo*[1,2], *Heon-Woo Kwon*[1,2], *Chang Hoon Yang*[1,2], *Jung-Sik Joo*[1,2], *Yong-Joon Cho*[3,4] *& Hyoung-Pyo Kim*[1,2,*]

[1]Department of Tropical Medicine, Institute of Tropical Medicine, Yonsei University College of Medicine, Seoul 03722, [2]Brain Korea 21 PLUS Project for Medical Science, Yonsei University College of Medicine, Seoul 03722, [3]Department of Molecular Bioscience, Kangwon National University, Chuncheon 24341, [4]Multidimensional Genomics Research Center, Kangwon National University, Chuncheon 24341, Korea

Trichomonas vaginalis **is an extracellular flagellated protozoan responsible for trichomoniasis, one of the most prevalent nonviral sexually transmitted infections. To persist in its host,** ***T. vaginalis*** **employs sophisticated gene regulation mechanisms to adapt to hostile environmental conditions. Although transcriptional regulation is crucial for this adaptation, the underlying molecular mechanisms remain poorly understood. Epigenetic regulation, particularly histone modifications, has emerged as a key modulator of gene expression. A previous study demonstrated that histone modifications, H3K4me3 and H3K27ac, promote active transcription. However, the complete extent of epigenetic regulation in** ***T. vaginalis*** **remains unclear. The present study extended these findings by exploring the repressive role of two additional histone H3 modifications, H3K9me3 and H3K27me3. Genome-wide analysis revealed that these modifications negatively correlated with gene expression, affecting protein-coding and transposable element genes (TEGs). These findings offer new insights into the dual role of histone modifications in activating and repressing gene expression and provide a more comprehensive understanding of epigenetic regulation in** ***T. vaginalis*****. This expanded knowledge may inform the development of novel therapeutic strategies targeting the epigenetic machinery of** ***T. vaginalis*****. [BMB Reports 2025; 58(2): 82-88]**

*Corresponding author. Tel: +82-2-2228-1842; Fax: +82-2-363-8676; E-mail: kimhp@yuhs.ac
#These authors contributed equally to this work.

https://doi.org/10.5483/BMBRep.2024-0175

Received 7 November 2024, Revised 24 November 2024, Accepted 12 December 2024, Published online 22 January 2025

Keywords: Chromatin, Epigenetic regulation, Histone modifications, Transcriptional repression, *Trichomonas vaginalis*

INTRODUCTION

Trichomonas vaginalis is a protozoan parasite responsible for trichomoniasis, the most common sexually transmitted disease of nonviral origin (1). This infection leads to vaginitis and urethritis in women and men, respectively. When this disease is contracted during pregnancy, it is associated with preterm delivery, low birth weight, and increased infant mortality (2). Chronic infection has also been implicated as a risk factor for the acquisition of human immunodeficiency virus (HIV), human papillomavirus (HPV), pelvic inflammatory disease, and increased predisposition to cervical and prostate cancers (3).

The *T. vaginalis* genome is unusually large for a protozoan, spanning approximately 160 megabases, and is highly repetitive, with nearly two-thirds of its content consisting of transposable elements (TEs) and repetitive sequences (4). This unique genomic composition enhances adaptability but requires robust regulatory mechanisms to mitigate potential disruptions in TE mobility (5). Although a high TE content may offer adaptive advantages under environmental pressures, stringent regulation is required to maintain genome stability (6, 7).

To establish and maintain infection, *T. vaginalis* must adapt its transcriptional profile (8). However, few core regulatory elements and transcription factors have been identified to date, leaving significant gaps in our understanding of the mechanisms that control gene expression during parasitic infection. Recently, there has been a growing interest in the epigenetic mechanisms involved in gene regulation within this parasite (9, 10). Notably, N6-methyladenine (6mA) has emerged as the primary methylation marker in the *T. vaginalis* genome, exhibiting a preference for TEs and intergenic regions, and is believed to play a role in modulating 3D chromatin architecture (10).

Histone modifications play a key role in shaping the chromatin structure and directing the recruitment of transcriptional machinery, thereby regulating essential cellular processes (11, 12). Song *et al*. provided the first direct evidence that histone modifications H3K4me3 and H3K27ac are crucial

ISSN: 1976-670X (electronic edition)

for active transcriptional regulation in *T. vaginalis* (9). However, the complete scope of the epigenetic regulation in this organism remains unclear. Based on previous findings, this study aimed to expand our understanding of *T. vaginalis* by investigating the repressive roles of two additional histone H3 modifications, H3K9me3 and H3K27me3, and their impact on gene expression to further clarify the various modes of chromatin-mediated gene regulation in this parasite.

RESULTS

Genome-wide mapping of histone marks H3K9me3 and H3K27me3 in *T. vaginalis*

To investigate whether *T. vaginalis* contains repressive histone modifications, its genome was first searched for genes encoding histone methyltransferase (HMT) enzymes that are evolutionarily conserved across species (13). Given the importance of H3K9me3 and H3K27me3 in repressive chromatin states across eukaryotes (14), the focus was on the HMTs associated with these markers. SUV39H1 is a well-known HMT responsible for the trimethylation of H3K9, a hallmark of heterochromatin and transcriptional silencing in many eukaryotes (15, 16). EZH2, a component of the polycomb repressive complex 2 (PRC2), catalyzes the trimethylation of H3K27, which is also associated with gene repression (17, 18). These enzymes play critical roles in maintaining cellular identity and in regulating gene expression during development (19, 20). Using the Trichomonas Genome Database (available from TrichDB at http://trichdb.org/trichdb) (21), several homologs of SUV39H1 and EZH2 in *T. vaginalis* were identified (Fig. 1A, B).

Next, RNA-sequencing (RNA-seq) data was generated and analyzed to assess the expression levels of these HMT genes in *T. vaginalis*. The analysis revealed that most of the identified HMTs were expressed at distinct levels, indicating that these enzymes are present and may play roles in histone methylation and transcriptional regulation within organisms (Fig. 1C, D).

To further confirm the presence and functional roles of these repressive histone modifications, chromatin immunoprecipitation was performed which was followed by high-throughput sequencing (ChIP-seq, chromatin immunoprecipitation sequencing) to map the genome-wide distribution of H3K9me3 and H3K27me3, along with the previously reported epigenetic markers H3K4me3 and H3K27ac (9, 22), across the *T. vaginalis* genome. A representative example of these distributions is shown in Fig. 1E, where distinct peaks corresponding to the repressive modifications, H3K9me3 and H3K27me3, were evident across the genome, confirming the presence of repressive chromatin states within the *T. vaginalis* genome. H3K4me3 and H3K27ac, which are typically associated with active transcription, were preferentially located in 5′ untranslated regions (UTRs) and intragenic coding sequences (Fig. 1F). In contrast, the repressive marks, H3K9me3 and H3K27me3, were uniformly distributed along the gene bodies, suggesting widespread repression of transcription across these regions (Fig. 1F).

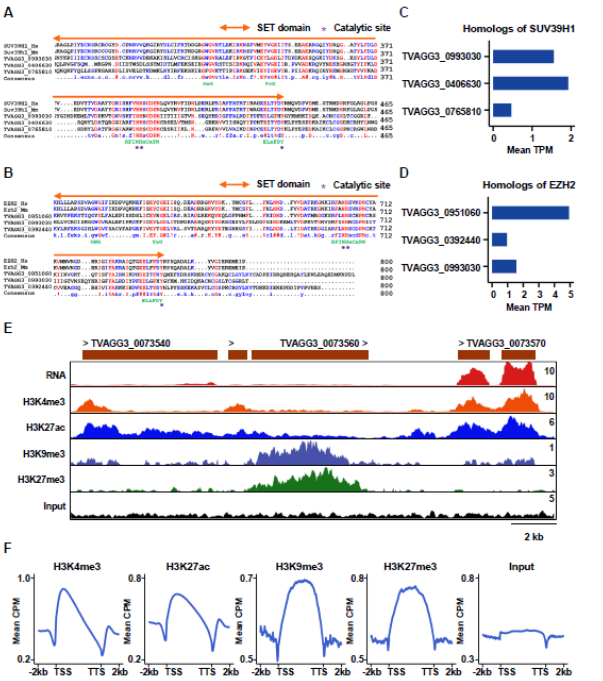

Fig. 1. Genome-wide mapping of RNA expression and histone modifications in *T. vaginalis*. Multiple protein sequence alignment of homologs of the (A) histone lysine methyltransferase SUV39H1 and (B) EZH2 with select orthologues. Alignments were performed with Multalin (http://bioinfo.genotoul.fr/multalin/). Gene bank accession numbers: human SUV39H1 (NP_001269095.1), mouse SUV39H1 (NP_035644.1), human EZH2 (NP_004447.2), and mouse EZH2 (NP_031997.2). Selected homologous regions are shown, with SET domains and catalytic sites indicated by arrows and asterisks. RNA-seq analysis reveals the expression of homologs of the (C) histone lysine methyltransferases SUV39H1 and (D) EZH2 in *T. vaginalis*, with the mean transcripts per million (TPM) for each homolog shown. (E) Genomic snapshot of the *TVAGG3_0073540* locus. Densities of RNA-seq reads and ChIP-seq reads for H3K4me3, H3K27ac, H3K9me3, H3K27me3, and input in *T. vaginalis* are shown. (F) Distribution of H3K4me3, H3K27ac, H3K9me3, H3K27me3, and input along gene length in all genes. TSS, transcription start site; TTS, transcription termination site; RNA-seq, RNA-sequencing; ChIP-seq, chromatin immunoprecipitation sequencing.

Association of H3K9me3 and H3K27me3 with repressive transcription in *T. vaginalis*

RNA expression and histone modification patterns, as observed in the genome tracks, suggested that transcriptional activity was associated with regions marked by H3K4me3 and H3K27ac. In contrast, the regions with H3K9me3 or H3K27me3 peaks exhibited little or no RNA expression (Fig. 1E). These findings indicated a strong association between active histone marks and transcriptional activity as well as a clear link between repressive marks and gene silencing. To better understand these relationships, the correlation between histone modifications and RNA expression across the entire *T. vaginalis*

genome was systematically analyzed, providing a comprehensive view of chromatin dynamics and transcriptional regulation in this organism.

The distribution of histone modification marks centered at transcription start sites (TSS) for all *T. vaginalis* genes were analyzed and categorized into quartiles based on their relative expression levels from RNA-seq data: top 25%, 25-50%, 50-75%, and 75-100%, along with a separate group of silent genes where no RNA sequencing reads were detected (Fig. 2A). Highly transcribed genes (top 25%) showed almost no H3K9me3 or H3K27me3, but exhibited strong enrichment of H3K4me3 and H3K27ac. In contrast, 62,601 silent genes displayed elevated levels of H3K9me3 and H3K27me3, with no detectable H3K4me3 or H3K27ac (Fig. 2A).

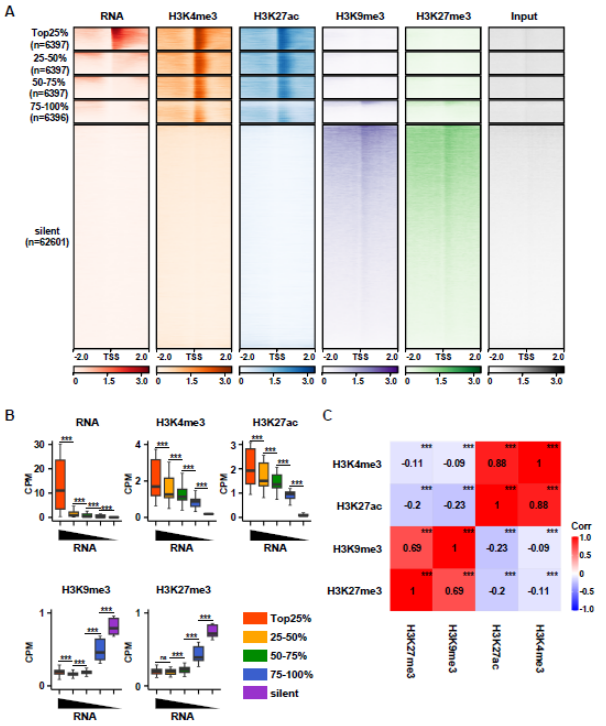

Fig. 2. Distinct histone modifications associated with active and repressive RNA expression in *T. vaginalis*. All genes were categorized into ranks based on RNA expression. Silent genes (rank 5), which have no RNA-seq reads, were identified separately, while the remaining genes were divided into ranks 1-4 according to their relative RNA expression (A and B). (A) Density heatmap shows coverages for RNA, H3K4me3, H3K27ac, H3K9me3, H3K27me3, and input across 4 kb centered at the TSS of each gene. (B) The enrichment of each histone modification across gene bodies (from TSS to TTS) for each gene group. Boxplot of relative levels of RNA, H3K4me3, H3K27ac, H3K9me3, and H3K27me3 for genes categorized by RNA expression. Significance determined by Kruskal Wallis test followed by Dunn post-hoc test. (***P $<$ 0.001). (C) Correlation matrix for histone modifications in *T. vaginalis*. This heatmap shows the pairwise correlation coefficients between histone modifications H3K4me3, H3K27ac, H3K9me3, and H3K27me3 across the *T. vaginalis* genome. Positive correlations are depicted in red, and negative correlations in blue, with color intensity representing the strength of the correlation. Significance determined by a student's t-test on the Spearman correlation coefficient. (***P $<$ 0.001). TSS, transcription start site; TTS, transcription termination site.

To further quantify these patterns, the enrichment of each histone modification across the gene bodies (from the TSS to the transcription termination site [TTS]) for each gene group was calculated. This permitted the direct comparison of active and repressive histone marks relative to gene expression levels. This analysis demonstrated that genes with the top 25% of expression exhibited significantly higher levels of H3K4me3 and H3K27ac markers associated with active transcription than genes with lower expression or silent genes (Fig. 2B). Conversely, silent and poorly expressed genes were enriched in H3K9me3 and H3K27me3, which is consistent with the role of these markers in transcriptional repression (Fig. 2B). These findings demonstrated a clear correlation between histone modifications and gene expression levels in *T. vaginalis*, with H3K9me3 and H3K27me3 being strongly linked to transcriptional silencing.

Cooperative and antagonistic roles of active and repressive histone modifications in the fine-tuning of RNA expression in *T. vaginalis*

H3K4me3 enrichment was strongly correlated with H3K27ac, whereas H3K9me3 showed a similarly high correlation with H3K27me3 (Fig. 2C). To explore these relationships further and investigate the cooperative and antagonistic roles of active and repressive histone modifications in regulating RNA expression in *T. vaginalis*, the genes were categorized into four ranks (1-4) based on their relative histone modification levels within the gene body, with rank 1 representing the highest level and rank 4 the lowest. By combining these rankings for both active (H3K4me3 and H3K27ac) and repressive (H3K9me3 and H3K27me3) modifications, 16 distinct gene groups were identified. RNA expression was then analyzed in each group using mean expression values and only genes with significant ChIP-seq signals (total normalized counts in gene bodies exceeding 0.1) were considered. The analysis revealed a clear pattern: enrichment of both active markers (H3K4me3 and H3K27ac), as did their RNA expression (Fig. 3A). Conversely, genes with elevated levels of the repressive markers (H3K9me3 and H3K27me3) exhibited significantly lower RNA expression levels (Fig. 3B).

In instances where an active mark demonstrated high enrichment and the corresponding repressive mark demonstrated low levels, gene expression levels were higher than in instances where repressive marks were also highly enriched (Fig. 3C-F). This indicated that active markers can counterbalance the effects of repressive markers, allowing for the nuanced regulation of gene expression. These findings demonstrated that active and repressive histone modification function both cooperatively and antagonistically to fine-tune RNA expression

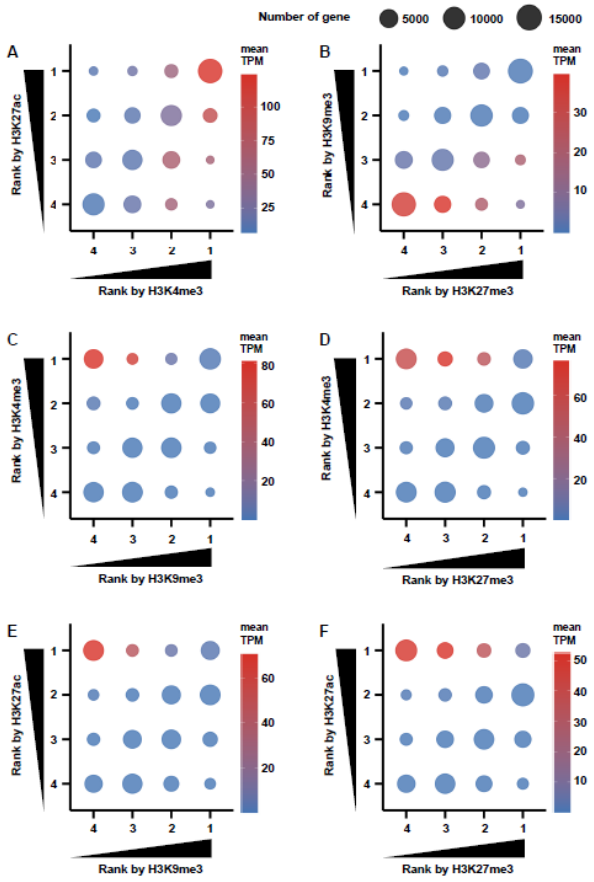

Fig. 3. Cooperative and antagonistic roles of active and repressive histone modifications in the fine-tuning of RNA expression in *T. vaginalis*. (A-F) Genes categorized into four ranks (ranks 1-4) according to their relative histone modification levels in the gene body. The size of the circles represents the number of genes, while the color densities indicate mean RNA expression.

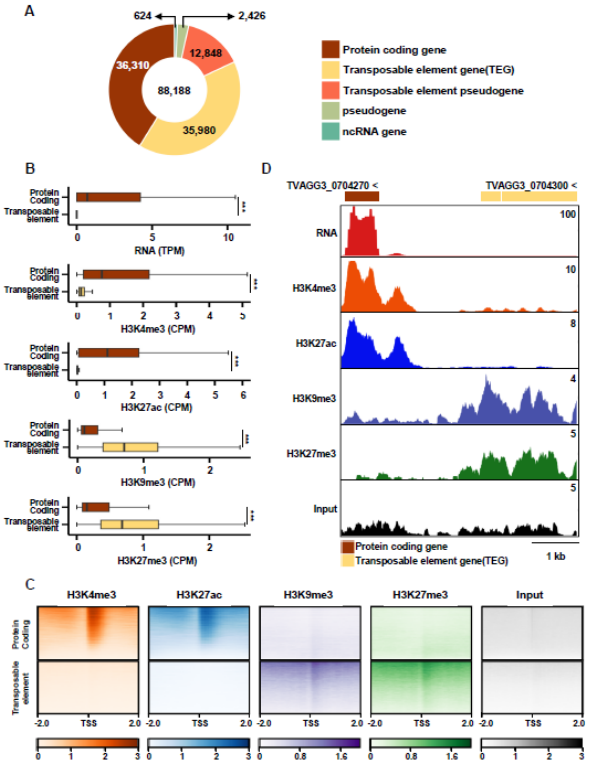

Fig. 4. The silenced expression of TEGs in *T. vaginalis* is associated with repressive histone modifications. (A) Pie charts of the number of protein-coding, TE, and other genes in *T. vaginalis*. (B) Boxplot of the relative levels of RNA, H3K4me3, H3K27ac, H3K9me3, and H3K27me3 for protein-coding genes, and TEGs. Significance determined by a student's t-test. (***P < 0.001). (C) Density heatmap shows distinct coverage analysis for protein-coding genes and transposable element genes, highlighting the levels of H3K4me3, H3K27ac, H3K9me3, H3K27me3, and input across a 4 kb window centered at the TSS of each gene. (D) The genomic snapshot of representative protein-coding genes and TEGs illustrates the densities of RNA-seq reads and ChIP-seq reads for H3K4me3, H3K27ac, H3K9me3, H3K27me3, and input. TEGs, transposable element genes; TE, transposable elements; RNA-seq, RNA-sequencing; ChIP-seq, chromatin immunoprecipitation sequencing.

in *T. vaginalis*. Active markers, such as H3K4me3 and H3K27ac, promote gene expression, whereas repressive markers, such as H3K9me3 and H3K27me3, suppress it. The interplay between these markers enables more precise control of transcriptional activity.

Distinct histone modifications maintain the silenced state of transposable element genes (TEGs) in *T. vaginalis*

The *T. vaginalis* genome was predicted to contain 88,188 genes including 36,310 and 35,980 protein-coding genes and TEGs, respectively (Fig. 4A). TEGs that can mobilize within the genome are typically repressed to avoid mutagenic effects (23-25). Unlike the protein-coding genes, which exhibited varying levels of RNA expression, the expression of TEGs is predominantly repressed (Fig. 4B, C). This repression was linked to the depletion of active histone markers, such as H3K4me3 and H3K27ac (Fig. 4B, C), along with the enrichment of repressive markers, including H3K9me3 and H3K27me3 (Fig. 4B, C). A clear example of this regulatory pattern is shown in Fig. 4D, where the actively transcribed gene *TVAGG3_0704270* was enriched with active markers (H3K4me3 and H3K27ac); however, the neighboring TEGs were depleted of these markers and showed enrichment of repressive markers (H3K9me3 and H3K27me3), maintaining their silenced state. These findings suggested that distinct histone modifications play a key regulatory role in maintaining the silenced state of TEGs while allowing for variable expression of protein-coding genes. This differential regulation may be crucial for adaptation and gene expression in *T. vaginalis*.

DISCUSSION

This study provides new insights into the role of histone modifications in regulating gene expression in *T. vaginalis*, emphasizing the dynamic interplay between active and repressive histone markers in fine-tuning RNA expression. The findings revealed that active markers (H3K4me3 and H3K27ac) and repressive markers (H3K9me3 and H3K27me3) function cooperatively or antagonistically, suggesting a sophisticated regulatory mechanism that supports diverse transcriptional outcomes across different gene categories in *T. vaginalis*.

The association between active histone markers, transcriptional activity, repressive markers, and gene silencing has been well-established in eukaryotes (26). This study confirms this relationship in *T. vaginalis*, where active markers are enriched in highly transcribed genes, and repressive markers are predominant in transcriptionally silent regions. This balance allows *T. vaginalis* to precisely regulate gene expression in response to changing environmental conditions, which is essential for its adaptation to its specific ecological niche. Further comparative studies with other eukaryotes could highlight how chromatin dynamics in *T. vaginalis* differ, enhancing our understanding of the unique regulatory strategies used by this organism.

TEGs are particularly abundant in *T. vaginalis*, underscoring their significance in the genome (4). Although TEGs contribute to genomic evolution and adaptability, their mobility can lead to genetic instability, potentially disrupting essential genes and cellular functions if not properly controlled (27, 28). This highlights the need for the strict regulation of TEGs in *T. vaginalis*, which has evolved multiple regulatory mechanisms to maintain its genomic integrity.

One major regulatory pathway involves DNA methylation, specifically at 6 mA, which is found predominantly near TEs and is linked to reduced TE expression (29-31). This epigenetic mark represses TEGs and plays a role in 3D genome organization, further influencing TE accessibility and activity. Another key mechanism involves small RNAs that target TEs, reduce RNA levels, and serve as silencing mechanisms to protect genomic stability (5, 32).

The results of this study highlighted histone modification as a crucial regulatory layer of TEGs in *T. vaginalis*. Active histone modification markers, H3K4me3 and H3K27ac, were significantly lower in the TEG regions, correlating with reduced TEG expression. Conversely, repressive markers, H3K9me3 and H3K27me3, were enriched around TEGs, further supporting their silenced states. This pattern suggests that histone modifications work in concert with small RNA and DNA methylation pathways, underscoring their essential roles in maintaining TEG repression and supporting genome stability in *T. vaginalis*.

Although this study provides valuable insights into the relationship between histone modifications and gene expression in *T. vaginalis*, certain limitations should be noted. The conclusions of this study are based on the correlations observed between the RNA-seq and ChIP-seq data, which indicate an association between histone marks and transcriptional activity. Functional experiments, such as the knockdown or overexpression of histone-modifying enzymes, would help establish a causal link between specific histone modifications and gene regulation.

While H3K9me3 and H3K27me3 are repressive histone marks, they likely play distinct roles in gene regulation. Due to the limitations of our current analysis, we could not fully explore these differences. Further investigation into their specific functions is crucial for advancing our understanding of their roles in gene regulation.

Another promising area for future research is the role of TEGs in determining genome structure and adaptability. Although TEGs are silenced, their potential for movement and creation of genomic variability could contribute to the adaptability of *T. vaginalis*. Investigating the conditions that activate TEGs and their effect on genome evolution can provide deeper insights into the adaptive strategies of organisms.

In conclusion, the findings of this study suggest that *T. vaginalis* employs a complex interplay between active and repressive histone modifications to regulate gene expression. This differential regulation of protein-coding genes and TEGs play a critical role in maintaining genomic stability, while allowing flexibility in gene expression. Understanding these mechanisms at greater depth could yield valuable insights into epigenetic regulation and offer potential therapeutic targets for controlling *T. vaginalis* infections.

MATERIALS AND METHODS

Cultivation of *T. vaginalis*

The T016 strain of *T. vaginalis* was axenically sub-cultivated at 37°C in Diamond's trypticase-yeast extract-maltose (TYM) medium with 10% heat-inactivated horse serum (Gibco, Invitrogen, Carlsbad, CA, USA) and 0.5% penicillin/streptomycin (Gibco). *T. vaginalis* cultures were supplemented with 50 μM 2'-2-bipyridyl (Sigma-Aldrich, St. Louis, MI, USA) for 18 h before RNA-seq and ChIP-seq library preparation.

RNA-seq

Total RNA from *T. vaginalis* was isolated using the Hybrid-R Total RNA Kit (GeneAll Biotechnology, Seoul, Korea). The RNA-seq library with three biological replicates was prepared using the TruSeq Stranded mRNA LT Sample Prep Kit (Illumina, San Diego, CA, USA). The libraries were sequenced on an Illumina HiSeq platform, generating 100-bp paired-end reads.

ChIP-seq

Cultures of *T. vaginalis* were washed once with PBS and fixed with 1% formaldehyde for 10 min at room temperature. Glycine (125 mM) was then added to stop the reaction. The

cells were incubated in swelling Buffer A (5 mM PIPES, pH 8.0, 85 mM KCl, 0.5% NP40) and subjected to sonication in Buffer A (10 mM Tris-HCl, pH 8.0, 2 mM EDTA, 0.2% SDS, protease inhibitors [Sigma-Aldrich], and 1 mM PMSF) using a Bioruptor sonication device (Diagenode, Liege, Belgium). Chromatin samples were diluted with Buffer B (10 mM Tris-HCl pH 8.0, 2% Triton X-100, 280 mM NaCl, 0.2% deoxycholate) and immunoprecipitated with antibodies specific for 1 μg H3K4me3, H3K27ac, H3K9me3, and H3K27me3 (Abcam, Cambridge, UK). Chromatin-antibody complexes were pulled down using Protein A/G Dynabeads (Invitrogen). The beads were washed twice with RIPA-140 (10 mM Tris-HCl pH 8.0, 1 mM EDTA, 140 mM NaCl, 1% Triton X-100, 0.1% SDS, and 0.1% deoxycholate), RIPA-300 (10 mM Tris-HCl pH 8.0, 1 mM EDTA, 300 mM NaCl, 1% Triton X-100, 0.1% SDS, and 0.1% deoxycholate), and LiCl Buffer (10 mM Tris-HCl pH 8.0, 1 mM EDTA pH 8.0, 250 mM LiCl, 0.5% deoxycholate, and 0.5% NP40). The beads were washed twice with cold 10 mM Tris-HCl (pH 8.0) to remove the detergents, salts, and EDTA. The Beads were then carefully resuspended in 25 μl of the tagmentation reaction mix containing 1 μl Tagment DNA Enzyme from the Nextera DNA Sample Prep Kit (Illumina) and incubated at 37℃ for 10 min in a thermocycler. The beads were washed twice with RIPA -140 and twice with cold TE buffer (10 mM Tris-HCl pH 8.0 and 0.1 mM EDTA) and then incubated with 70 μl elution buffer (0.4% SDS, 300 mM NaCl, 5 mM EDTA, 1% Triton X-100, and 10 mM Tris-HCl pH 8.0) containing 2 μl of Proteinase K (NEB) for 1 h at 55°C and 8 h at 65°C, to revert formaldehyde cross-linking. The resulting supernatant was transferred to a new tube. Finally, DNA was purified using SPRI AMPure XP beads (sample-to-bead ratio of 1:1.8). The libraries were sequenced on an Illumina HiSeq platform, generating 100-bp paired-end reads. Two biological replicates were used for each experiment.

RNA-Seq data processing

Paired-end sequence reads were trimmed to remove adaptor sequences and low-quality bases using TrimGalore v0.6.8dev and Cutadapt v4.1 (33). The trimmed reads were mapped to the *T. vaginalis* genome downloaded from TrichDB v68 (https://trichdb.org/trichdb/app/) using STAR v2.7.10a (34) with –sjdbGTFtagExonParentTranscript Parent and –twopassMode Basic options. The expression level of each transcript was estimated using RSEM v1.3.1 (35), with –estimate-rspd –paired-end option. Bigwig files were generated from BAM files using deep tools v3.5.3 (36) bamCoverage function with –normalization using the CPM option and visualized with PyGenomeTracks v3.6 (37).

ChIP-Seq data processing

Paired-end sequencing reads were trimmed to remove adaptor sequences and low-quality bases using Trimm Galore v0.6.8dev and Cutadapt v4.1. Trimmed reads were mapped to TrichDB v68 using bwa v0.7.17 (38) with default options. Duplicate reads were removed using PICARD v2.18.23. Peaks were called using macs2 v2.2.7.1 (39) with an input reference bam file of -f BAMPE -g 181470000. H3K27me3 and H3K9me3 ChIP-seq peaks were identified using –broad option for a broad profile. Normalized Bigwig files were generated using deeptools v3.5.3 function bamCoverage with the same parameters as the RNA-seq analysis, and visualized with PyGenomeTracks v3.6. Categorized ChIP-seq heatmaps were generated using deepTools with option "computeMatrix reference-point TSS -a 2000 -b 2000 –missingDataAsZero."

Multiple sequence alignment

Homologous genes of histone lysine methyltransferase EZH2 and SUV39H were identified using the basic local alignment search tool (BLAST) (13) in TrichDB v68, and multiple sequence alignment of the top three genes was performed using Multalin (http://bioinfo.genotoul.fr/multalin/) (40).

Data access

The RNA-seq and ChIP-seq data used in this study have been deposited in the Gene Expression Omnibus (GEO) under accession numbers GSE279415 (https://www.ncbi.nlm.nih.gov/geo/query/acc.cgi?acc=GSE279415) and GSE279416 (https://www.ncbi.nlm.nih.gov/geo/query/acc.cgi?acc=GSE279416).

ACKNOWLEDGEMENTS

This work was supported by the National Research Foundation of Korea (NRF) grants funded by the Korean government (MSIP) (2020R1A2C2013258, and 2022M3A9B6017424 to H.-P. Kim).

CONFLICTS OF INTEREST

The authors have no conflicting interests.

REFERENCES

1. Shiratori M, Patel A, Gerhold RW, Sullivan SA and Carlton JM (2023) Persistent Trichomonas vaginalis infections and the pseudocyst form. Trends Parasitol 39, 1023-1031
2. Fichorova RN (2009) Impact of T. vaginalis infection on innate immune responses and reproductive outcome. J Reprod Immunol 83, 185-189
3. Schwebke JR and Burgess D (2004) Trichomoniasis. Clin Microbiol Rev 17, 794-803
4. Carlton JM, Hirt RP, Silva JC et al (2007) Draft genome sequence of the sexually transmitted pathogen Trichomonas vaginalis. Science 315, 207-212
5. Warring SD, Blow F, Avecilla G, Orosco JC, Sullivan SA and Carlton JM (2021) Small RNAs are implicated in regulation of gene and transposable element expression in the protist trichomonas vaginalis. mSphere 6, e01061-20

6. Biemont C and Vieira C (2006) Genetics: junk DNA as an evolutionary force. Nature 443, 521-524
7. Oliver KR and Greene WK (2009) Transposable elements: powerful facilitators of evolution. Bioessays 31, 703-714
8. Figueroa-Angulo EE, Rendón-Gandarilla FJ, Puente-Rivera J et al (2012) The effects of environmental factors on the virulence of Trichomonas vaginalis. Microbes Infect 14, 1411-1427
9. Song MJ, Kim M, Choi Y et al (2017) Epigenome mapping highlights chromatin-mediated gene regulation in the protozoan parasite Trichomonas vaginalis. Sci Rep 7, 45365
10. Lizarraga A, O'Brown ZK, Boulias K et al (2020) Adenine DNA methylation, 3D genome organization, and gene expression in the parasite Trichomonas vaginalis. Proc Natl Acad Sci U S A 117, 13033-13043
11. Millán-Zambrano G, Burton A, Bannister AJ and Schneider R (2022) Histone post-translational modifications - cause and consequence of genome function. Nat Rev Genet 23, 563-580
12. Lee SH, Li Y, Kim H, Eum S, Park K and Lee CH (2022) The role of EZH1 and EZH2 in development and cancer. BMB Rep 55, 595-601
13. Boratyn GM, Camacho C, Cooper PS et al (2013) BLAST: a more efficient report with usability improvements. Nucleic Acids Res 41, W29-W33
14. Bannister AJ and Kouzarides T (2011) Regulation of chromatin by histone modifications. Cell Res 21, 381-395
15. Rea S, Eisenhaber F, O'Carroll D et al (2000) Regulation of chromatin structure by site-specific histone H3 methyltransferases. Nature 406, 593-599
16. Ninova M, Fejes Toth K and Aravin AA (2019) The control of gene expression and cell identity by H3K9 trimethylation. Development 146, dev181180
17. Trojer P and Reinberg D (2007) Facultative heterochromatin: is there a distinctive molecular signature? Mol Cell 28, 1-13
18. Di Croce L and Helin K (2013) Transcriptional regulation by Polycomb group proteins. Nat Struct Mol Biol 20, 1147-1155
19. Jiang L, Huang L and Jiang W (2024) H3K27me3-mediated epigenetic regulation in pluripotency maintenance and lineage differentiation. Cell Insight 3, 100180
20. Nicetto D and Zaret KS (2019) Role of H3K9me3 heterochromatin in cell identity establishment and maintenance. Curr Opin Genet Dev 55, 1-10
21. Aurrecoechea C, Brestelli J, Brunk BP et al (2009) GiardiaDB and TrichDB: integrated genomic resources for the eukaryotic protist pathogens Giardia lamblia and Trichomonas vaginalis. Nucleic Acids Res 37, D526-D530
22. Park PJ (2009) ChIP-seq: advantages and challenges of a maturing technology. Nat Rev Genet 10, 669-680
23. Mc CB (1950) The origin and behavior of mutable loci in maize. Proc Natl Acad Sci U S A 36, 344-355
24. Deniz O, Frost JM and Branco MR (2019) Regulation of transposable elements by DNA modifications. Nat Rev Genet 20, 417-431
25. Bruno M, Mahgoub M and Macfarlan TS (2019) The arms race between krab-zinc finger proteins and endogenous retroelements and its impact on mammals. Annu Rev Genet 53, 393-416
26. Zhang T, Cooper S and Brockdorff N (2015) The interplay of histone modifications - writers that read. EMBO Rep 16, 1467-1481
27. Bourque G, Burns KH, Gehring M et al (2018) Ten things you should know about transposable elements. Genome Biol 19, 199
28. Kazazian HH Jr. and Moran JV (2017) Mobile DNA in health and disease. N Engl J Med 377, 361-370
29. Wion D and Casadesus J (2006) N6-methyl-adenine: an epigenetic signal for DNA-protein interactions. Nat Rev Microbiol 4, 183-192
30. Wu TP, Wang T, Seetin MG et al (2016) DNA methylation on N(6)-adenine in mammalian embryonic stem cells. Nature 532, 329-333
31. Chen H, Shu H, Wang L et al (2018) Phytophthora methylomes are modulated by 6mA methyltransferases and associated with adaptive genome regions. Genome Biol 19, 181
32. Saito K and Siomi MC (2010) Small RNA-mediated quiescence of transposable elements in animals. Dev Cell 19, 687-697
33. Martin M (2011) Cutadapt removes adapter sequences from high-throughput sequencing reads. EMBnet Journal 17, 10-12
34. Dobin A, Davis CA, Schlesinger F et al (2013) STAR: ultrafast universal RNA-seq aligner. Bioinformatics 29, 15-21
35. Li B and Dewey CN (2011) RSEM: accurate transcript quantification from RNA-Seq data with or without a reference genome. BMC Bioinformatics 12, 323
36. Ramirez F, Dundar F, Diehl S, Gruning BA and Manke T (2014) deepTools: a flexible platform for exploring deep-sequencing data. Nucleic Acids Res 42, W187-W191
37. Lopez-Delisle L, Rabbani L, Wolff J et al (2021) pyGenomeTracks: reproducible plots for multivariate genomic datasets. Bioinformatics 37, 422-423
38. Li H and Durbin R (2009) Fast and accurate short read alignment with Burrows-Wheeler transform. Bioinformatics 25, 1754-1760
39. Zhang Y, Liu T, Meyer CA et al (2008) Model-based analysis of ChIP-Seq (MACS). Genome Biol 9, R137
40. Corpet F (1988) Multiple sequence alignment with hierarchical clustering. Nucleic Acids Res 16, 10881-10890